

Bulk modulus and high-pressure crystal structures of tetrakis(trimethylsilyl)methane $C[Si(CH_3)_3]_4$ determined by X-ray powder diffraction

Robert E. Dinnebier,^{a*} Stefan Carlson^b and Sander van Smaalen^a

^aLaboratory of Crystallography, University of Bayreuth, D-95440 Bayreuth, Germany, and

^bHigh Pressure Group, ESRF, BP 220, F-38043 Grenoble CEDEX, France

Correspondence e-mail:
robert.dinnebier@uni-bayreuth.de

Received 15 September 1999

Accepted 1 November 1999

The pressure dependence of the crystal structure of cubic tetrakis(trimethylsilyl)methane $C[Si(CH_3)_3]_4$ (TC) ($P < 16.0$ GPa, $T = 298$ K) is reported using high-resolution angle-dispersive X-ray powder diffraction. The compound has crystal structures with the molecules in a cubic-close-packed (c.c.p.) arrangement. It shows three phase transitions in the measured pressure range. At ambient conditions, TC has space group $Fm\bar{3}m$ ($Z = 4$) with $a = 12.8902(2)$ Å, $V = 2141.8(1)$ Å³ (phase I). Between 0 and 0.13 GPa TC exhibits a first-order phase transition into a structure with space group $Pa\bar{3}$ (phase II). A second first-order phase transition occurs between 0.2 and 0.28 GPa into a structure with space group $P2_13$ (phase III). Under non-hydrostatic pressure conditions ($P > 10$ GPa) a transformation is observed into a c.c.p. structure that is different from the face-centred-cubic structure at ambient conditions. A non-linear compression behaviour is observed, which could be described by a Vinet relation in the range 0.28–4.8 GPa. The extrapolated bulk modulus of the high-pressure phase III was determined to be $K_0 = 7.1(8)$ GPa. The crystal structures in phase III are refined against X-ray powder data measured at several pressures between 0.49 and 4.8 GPa, and the molecules are found to be fully ordered. This is interpreted to result from steric interactions between neighbouring molecules, as shown by analysing the pressure dependence of intramolecular angles, torsion angles and intermolecular distances. Except for their cell dimensions, phases I, II and III are found to be isostructural to the corresponding phases at low temperatures.

1. Introduction

The compound tetrakis(trimethylsilyl)methane $C[Si(CH_3)_3]_4$ (TC) belongs to a class of crystalline molecular compounds with non-polar almost spherically shaped molecules in a close-packed stacking (Fig. 1). Solid-state NMR studies (Dereppe & Magill, 1972; Aliev *et al.*, 1993, 1994; Helluy *et al.*, 1998) have established that at room temperature the molecules in crystalline TC undergo rapid (kHz scale) reorientational jumps about fixed centres of mass forming so-called 'rotator-phases' or 'plastic' crystals (Parsonage & Staveley, 1978).

The molecular structure of TC in the gas phase has been determined by electron diffraction (Beagley *et al.*, 1988, 1989). In the gas phase the molecule has $23(T)$ symmetry, with $\sim 18^\circ$ cooperative twisting of the trimethylsilyl groups from a fully extended staggered T_d configuration to reduce steric hindrance between methyl groups. This conformation has been corroborated by force-field calculations (Iroff & Mislow, 1978; Beagley *et al.*, 1988). The high symmetry of the free

molecules is retained in the solid state at room temperature, where the crystal structure of TC has space group $Fm\bar{3}m$ with molecules showing approximately sixfold orientational disorder (Dereppe & Magill, 1972; Dinnebier *et al.*, 1999). Upon cooling, TC undergoes two first-order phase transitions into structures of increasing order, as evidenced by X-ray powder diffraction, differential scanning calorimetry and NMR (Dinnebier *et al.*, 1999). The phase transitions occur at 268 K into a structure with space group $Pa\bar{3}$ and with twofold disorder of the molecules, and at 225 K into a fully ordered structure with space group $P2_13$ (Fig. 4).

In this work we have investigated the pressure dependence of the crystal structure of TC. For this purpose, *in situ* X-ray powder diffraction measurements were performed at room temperature and elevated pressures using a diamond anvil cell (DAC).

2. Experimental

2.1. Sample preparation

Our sample of TC was kindly donated by G. Fritz, Karlsruhe. The polycrystalline samples consisted of fine equidimensional colourless grains without discernible facets. They are stable in air. Owing to the softness of the material, grinding was not possible and instead a razor blade was used to produce a finely powdered sample.

2.2. X-ray diffraction measurements

For the X-ray powder diffraction experiments the sample was loaded into a membrane-driven DAC (Letoulec *et al.*, 1988) with silicon oil as the pressure medium. The DAC was

equipped with 600 μm culet diamonds and stainless-steel gaskets with 250 μm -diameter holes. The pressure was determined by the ruby luminescence method using the wavelength shift calibration of Mao *et al.* (1986). High-pressure X-ray powder diffraction data were collected at room temperature at beamline ID30 of the European Synchrotron Radiation Facility (ESRF). Monochromatic radiation for the high-pressure experiment was selected at 29.200 keV (0.4246 \AA). A (111) channel-cut Si monochromator, operated in vacuum (water-cooled), was irradiated by synchrotron radiation from two phased undulators of period 40 mm. The X-ray beam, with an initial size 0.3×0.3 mm after the monochromator, was collimated down to a FWHM of 0.080×0.080 mm using tungsten carbide slits.

An angle-dispersive powder diffraction technique with an online fast-readout two-dimensional image-plate detector (Thoms *et al.*, 1998) was used. Exposure times between 20 and 25 min were chosen. Data reduction was performed using the program *FIT2D* (Hammersley *et al.*, 1998), resulting in diagrams of corrected intensities *versus* the scattering angle 2θ . It was observed that the diffracted intensity was quite uniformly distributed over the Debye–Scherrer rings, ruling out severe grain size effects and preferred orientation.

2.3. LeBail and Rietveld refinements

The dependence of the scattering profile on pressure provides evidence for three first-order phase transitions (Fig. 2). The phase (phase I) with symmetry $Fm\bar{3}m$ which is stable at ambient conditions is retained up to at least 0.07 GPa. A transition into a phase with symmetry $Pa\bar{3}$ (phase II) is observed to occur between 0.07 and 0.13 GPa. Above 0.28 GPa and at least up to 4.8 GPa a structure is stable with symmetry $P2_13$ (phase III). Owing to the freezing of the pressure medium at ~ 5 GPa, non-hydrostatic conditions were met above this pressure. On increasing pressure, broadening of the diffraction maxima was observed, and peaks shifted towards positions that did not conform to any lattice. Nevertheless, at pressures above 10 GPa the diffraction profile was found to contain only maxima corresponding to a face-centred-cubic (f.c.c.) lattice (phase IV), and a fourth phase was thus confirmed to be present under these conditions.

The powder patterns of phase I and of phase II (Fig. 3) are characterized by a rapid fall-off of the diffracted intensity with increasing scattering angle indicating rotational disorder of the TC molecules (Dinnebier *et al.*, 1999). The information contained in these scattering profiles appeared to

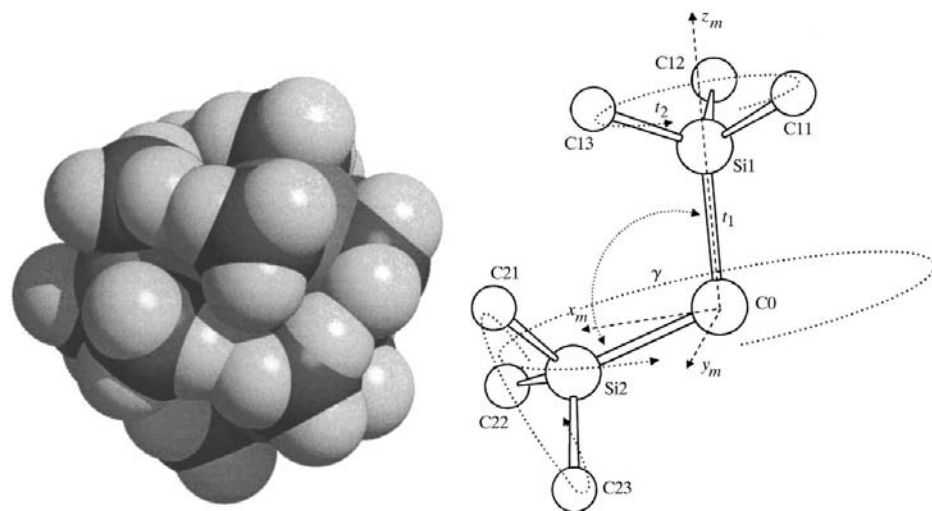


Figure 1

Left: cup model of TC in the conformation attained in the crystal at a pressure of 4.8 GPa with the H atoms at calculated positions. Right: ball-and-stick model of TC [only the central C atom, C0, and the two crystallographically independent trimethylsilyl groups, (Si1, C11, C12, C13) and (Si2, C21, C22, C23), are shown]. Indicated are the bond lengths l_1 and l_2 , the molecular coordinate system $\{x_m, y_m, z_m\}$, and the tetrahedral angle $\gamma = 109.471^\circ$. The molecular z_m axis corresponds to the 111 axis of the crystallographic coordinate system. Three orientational degrees of freedom were refined: rotation of the first trimethylsilyl group around the C0–Si1 bond, rotation of the second trimethylsilyl group around the C0–Si2 bond, and rotation of the second trimethylsilyl group around the C0–Si1 bond.

be insufficient to refine the crystal structures, but it could be used to obtain accurate values for the cubic lattice parameters by full-profile fitting using the LeBail method. The powder patterns of phase III (e.g. Fig. 3c) contain a sufficient amount of resolved diffraction peaks to allow Rietveld refinements of the structures. A more detailed analysis of phase IV was not possible, owing to the poor quality of the data.

The program package *GSAS* (Larson & Von Dreele, 1994) was used for all refinements. For all phases in the pressure range between 0.07 and 4.8 GPa (phases I, II and III), precise lattice and reflection profile parameters were determined using the LeBail full-profile refinement technique. Low-angle peaks of phase I had a full width at half-maximum of 0.04° in 2Θ , which is close to the instrumental resolution. The background was modelled manually. The peak profile was described by a pseudo-Voigt function (Thompson *et al.*, 1987). To account for the barely detectable peak asymmetry, an empirical function as implemented in *GSAS* (profile function #2) was used.

For the Rietveld refinements the lattice and reflection profile parameters were kept at the values as obtained from the LeBail fit. The single independent molecule was placed at the origin with one of the bonds, C–Si1, directed along the threefold $\langle 111 \rangle$ axis. Using space-group symmetry only, there are seven independent non-H atoms with a total of 16 independent positional parameters. To account for the contribution to the scattering power of the H atoms of the methyl groups, the occupation values of the C atoms were set to 1.5, as discussed by Dinnebier *et al.* (1999). Unconstrained refinement of the positional parameters of the non-H atoms using the starting coordinates of the corresponding low-temperature phases (Dinnebier *et al.*, 1999) did not converge due to the

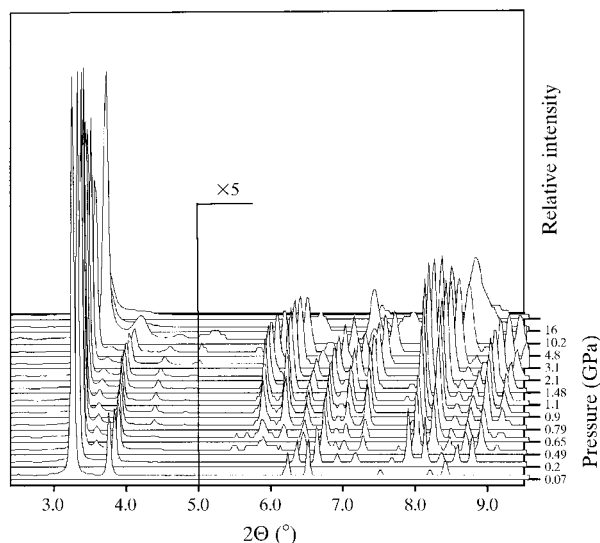


Figure 2 Scattered X-ray intensity of TC as a function of diffraction angle 2Θ and pressure. The wavelength was $\lambda = 0.4246 \text{ \AA}$. Phases identified are in order of increasing pressure: $Fm\bar{3}m$ ($0 < P \leq 0.07 \text{ GPa}$), $Pa\bar{3}$ ($0.13 \leq P \leq 0.2 \text{ GPa}$), $P2_13$ ($0.28 \leq P \leq 4.8 \text{ GPa}$), f.c.c. ($P \geq 10.2 \text{ GPa}$). The two peaks at approximately $5.5^\circ 2\Theta$ and pressures $< 1 \text{ GPa}$ are due to scattering of the DAC. The higher-angle part starting at $5^\circ 2\Theta$ is enlarged by a factor of five. Note that the pressure scale is non-linear.

Table 1 Rigid-body coordinates of a trimethylsilyl group with the origin located at the central C0 atom.

The multipliers t_1 and t_2 for the two vectors needed to build the rigid body are equivalent to the Si–C bond length (from Dinnebier *et al.*, 1999).

	$t_1 = 1.89$			$t_2 = 1.89$		
Si1	0	0	1	0	0	0
C11	0	0	1	$(2)^{1/2}/3$	$-(2)^{1/2}/3$	1/3
C12	0	0	1	0	$2(2)^{1/2}/3$	1/3
C13	0	0	1	$-2(2)^{1/2}/3$	$-(2)^{1/2}/3$	1/3

reduced amount of information in the X-ray powder diffraction pattern at high pressure. Instead, two rigid bodies were used, representing the two crystallographic independent trimethylsilyl groups (Table 1, Fig. 1). With the tetrahedral angle between the two rigid bodies kept at 109.47° , and fixing the average Si–C bond length at 1.889 \AA (Bartell *et al.*, 1970), the number of refinable parameters was reduced to three rotations. These can be described as follows: rotation φ of the entire TC molecule around $\langle 111 \rangle$, rotation ϕ_1 of the trimethylsilyl group on the $\langle 111 \rangle$ axis about this axis, and rotation ϕ_2 of the second trimethylsilyl group about its C–Si2 bond. The tetrahedral angle between the two trimethylsilyl groups was released at the final stage of the refinement process, but it did not change significantly. A single overall temperature factor for the TC molecule was refined. The final weighted profile R_{wp} converged to values close to that of the best LeBail fits.¹

3. Results and discussion

X-ray scattering on TC at various pressures has provided the lattice parameters as a function of pressure. From these results the pressure dependence of the relative volume has been derived (Fig. 4). Whereas the volume V decreases at most by 3.5% with temperature (Dinnebier *et al.*, 1999), it decreases by 23.5% at 4.8 GPa, indicating a very soft and highly compressible material. The volume/pressure relation represents the equation of state (EoS), which can be described analytically by series expansions of Eulerian finite strain (Birch–Murnaghan EoS) or cohesive energies in a condensed system (Vinet EoS). The data for phase III could be adequately fitted to several widely used EoS using the program *EOSFIT* (Angel, 1999). The best results were obtained by the Vinet EoS (Vinet *et al.*, 1986) defined as

$$P = 3K_0 \frac{(1 - f_v)}{f_v^2} \exp\left[\frac{3}{2}(K' - 1)(1 - f_v)\right], \quad (1)$$

where $f_v = (V/V_0)^{1/3}$, with the volume at zero pressure V_0 , the bulk modulus K_0 , and its pressure derivative at zero pressure and ambient temperature K' . Alternatively, the data were

¹ Supplementary data for this paper are available from the IUCr electronic archives (Reference: SE0299). Services for accessing these data are described at the back of the journal.

fitted with the third-order truncation of the Birch–Murnaghan EoS (BM3 EoS) (Birch, 1947) defined as

$$P = 3K_0 f_E (1 + 2f_E)^{5/2} \left[1 + \frac{3}{2}(K' - 4)f_E \right], \quad (2)$$

where $f_E = [(V_0/V)^{2/3} - 1]/2$. The results are given in Table 2. Both EoS yield the same values within their standard deviations. All parameters show high correlation (>88%) between each other. Two lines drawn through the volume data in Fig. 4 represent the fitted Vinet (solid line) and Birch–Murnaghan EoS (dotted line), respectively. Differences between the two EoS are apparent only in the extrapolated part before the first data point at 0.28 GPa, affecting the value of the extrapolated bulk modulus. Since the Vinet EoS is believed to yield more accurate parameters for highly compressible materials (Angel

Table 2

Parameters of different equations of state (EoS) for the high-pressure phase III of TC obtained by least-squares fits.

	V_0 (Å ³)	K_0 (GPa)	K'
Vinet EoS	2066 (11)	7.1 (8)	10.1 (8)
BM3 EoS	2081 (17)	5.5 (13)	15.0 (34)

& Vaughan, 2000), we use the values determined by this function.

For phase I, only one data point exists, from which no information about the compressibility of this phase can be obtained. For phase II, two data points exist, which allowed the slope to be determined from a linear interpolation between them. The higher slope of the volume on pressure relation for phase II indicates a higher compressibility and therefore a lower bulk modulus in comparison with the corresponding values of phase III. This behaviour can be explained by the smaller packing effect of the dynamically disordered TC molecules at low pressure.

The data of the relative volume in dependence of temperature (Dinnebier *et al.*, 1999) were fitted to empirical functions of the type

$$\frac{V}{V_0}(T) = [P1 + P2(295 - T)]^{P3}, \quad (3)$$

with $P1 = 1.022$ (3), $P2 = -0.013$ (3) and $P3 = 0.0080$ (2) for the high-temperature phase, $P1 = -0.2$ (8), $P2 = 0.12$ (5) and $P3 = -0.0067$ (10) for the intermediate-temperature phase,

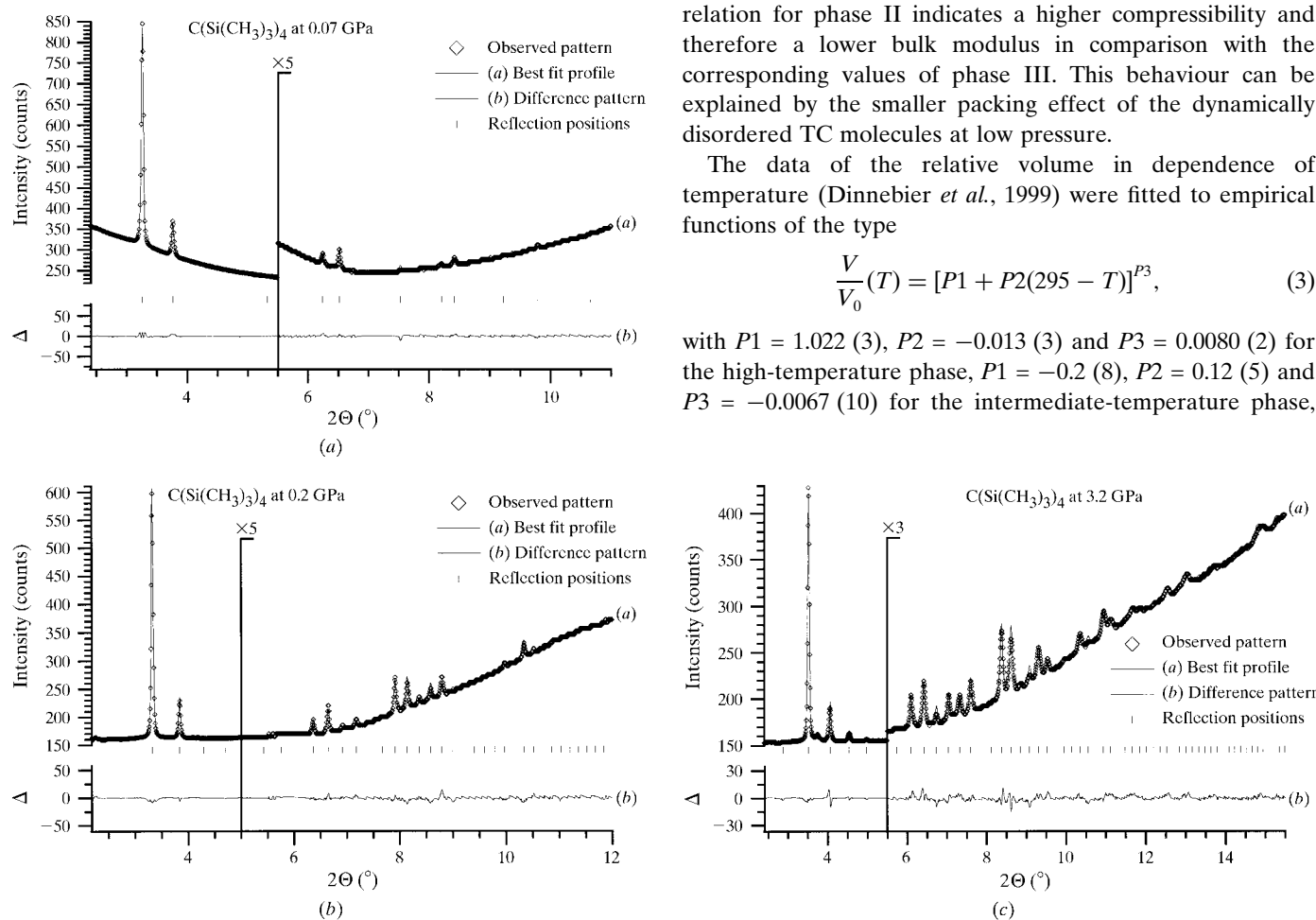


Figure 3

(a) Scattered X-ray intensity for the low-pressure phase of TC at $P = 0.07$ GPa as a function of diffraction angle 2θ . Shown are the observed pattern (diamonds), the best LeBail-fit profile in $Fm\bar{3}m$ (line *a*), the difference curve between observed and calculated profile (line *b*), and the reflection markers (vertical bars). The wavelength was $\lambda = 0.4246$ Å. The higher-angle part starting at 5.5° 2θ is enlarged by a factor of five. The R values are $R_p = 1.8\%$, $R_{wp} = 3.0\%$. Steps in the measured profile are due to round-off effects resulting from digitalization of the image plate. (b) Scattered X-ray intensity for the intermediate-pressure phase of TC at $P = 0.2$ GPa as a function of diffraction angle 2θ . Shown are the observed pattern (diamonds), the best LeBail-fit profile in $Pa\bar{3}$ (line *a*), the difference curve between observed and calculated profile (line *b*), and the reflection markers (vertical bars). The wavelength was $\lambda = 0.4246$ Å. The higher-angle part starting at 5.5° 2θ is enlarged by a factor of five. The R values are $R_p = 2.9\%$, $R_{wp} = 4.7\%$. Steps in the measured profile are due to round-off effects resulting from digitalization of the image plate. (c) Scattered X-ray intensity for the high-pressure phase of TC at $P = 3.2$ GPa as a function of diffraction angle 2θ . Shown are the observed pattern (diamonds), the best Rietveld-fit profile in $P2_13$ (line *a*), the difference curve between observed and calculated profile (line *b*), and the reflection markers (vertical bars). The wavelength was $\lambda = 0.4246$ Å. The higher-angle part starting at 5.5° 2θ is enlarged by a factor of three. The R values are $R_p = 4.5\%$, $R_{wp} = 7.7\%$ and $R(F^2) = 18.5\%$. Steps in the measured profile are due to round-off effects resulting from digitalization of the image plate.

and $P1 = -5$ (3), $P2 = 0.21$ (7) and $P3 = -0.0081$ (6) for the low-temperature phase.

Owing to the disorder and the limited amount of data, the molecular conformations in phases I and II could not be determined from the X-ray experiments. From the extinction rules and the similarity of the powder patterns of phases I, II and III at high pressure to their counterparts at low temperature, it may be concluded that they are isostructural.

The high quality of the powder patterns of phase III permitted rigid-body Rietveld refinements and therefore allowed the determination of structural parameters in dependence on pressure. Under the assumption that the bond distances between C and Si atoms as well as the tetrahedral angle between the four trimethylsilyl groups do not depend on pressure, three intramolecular degrees of freedom remained, which were refined. All three parameters (φ , ϕ_1 , ϕ_2) show a high correlation with respect to the temperature factor for pressures below 0.9 GPa and an almost linear dependence on pressure between 0.9 and 4.8 GPa (Fig. 5).

The rotation φ of the base plane of the Si_4 tetrahedron of the TC molecule around the [111] axis increases slightly with pressure, which could be described by the linear relationship φ ($^\circ$) = $13.386 + 0.560P$ (GPa). A cooperate-twist of 18° for TC of the trimethylsilyl groups from the reference (ecliptic) T_d structure was found by electron diffraction studies in the gas phase (Beagley *et al.*, 1988, 1989). It was shown previously (Dinnebier *et al.*, 1999) that at temperatures below 225 K an improved packing was achieved by different twist angles for the two independent trimethylsilyl groups, leading to $3(C3)$ symmetry for the TC molecules. At 150 K the two crystallographically independent trimethylsilyl groups were found to

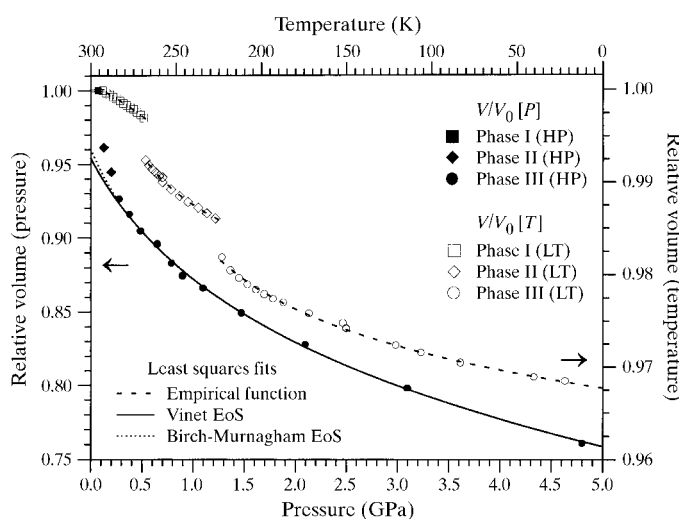


Figure 4 Dependence of the relative volume of TC on pressure in the range 0–5.0 GPa (this work) and temperature in the range 25–300 K (Dinnebier *et al.*, 1999). The three phases at high pressure are marked by three different filled symbols. The three phases at low temperature are marked by open symbols. The solid and the dotted line correspond to least-squares fits of a Vinet and a Birch–Murnaghan equation of state, respectively. Differences between the two fitting functions are visible in the extrapolated pressure range below 0.28 GPa. Note the offset of the two scales of the relative volume parameter.

assume different twists of $\phi_1 = 14.4$ and $\phi_2 = 20.3^\circ$, respectively. Presently we have determined that in the isosymmetric high-pressure phase these two twist angles ϕ_1 and ϕ_2 are pressure-dependent according to ϕ_1 ($^\circ$) = $37.448 - 2.314P$ (GPa) for the trimethylsilyl group oriented along the [111] direction and ϕ_2 ($^\circ$) = $20.906 + 0.061P$ (GPa) for the second trimethylsilyl group. For increasing pressure the difference between the twist angles becomes smaller. It may be speculated that eventually they become equal, or the transition into phase IV occurs earlier (Fig. 5).

The structural parameters obtained at different temperatures or different pressures can all be described as a function of the volume of the unit cell. However, this does not lead to a simplified description of the twist angles in the low-temperature structure and the twist angles obtained at high pressure. One reason not to expect such a relation is that the lattice parameter of phase III at the lowest pressure for which phase III occurs is already smaller than the low-temperature value (Fig. 4). One may speculate that in the regime of compression down to 95% of the volume of the unit cell at ambient conditions the structural changes are large, and that they do not follow the quasi-linear dependence observed at high pressures. This idea is in accordance with the strong decay of the twist angles at low pressure (<0.49 GPa). It may be assumed that in the two disordered phases I and II a similar

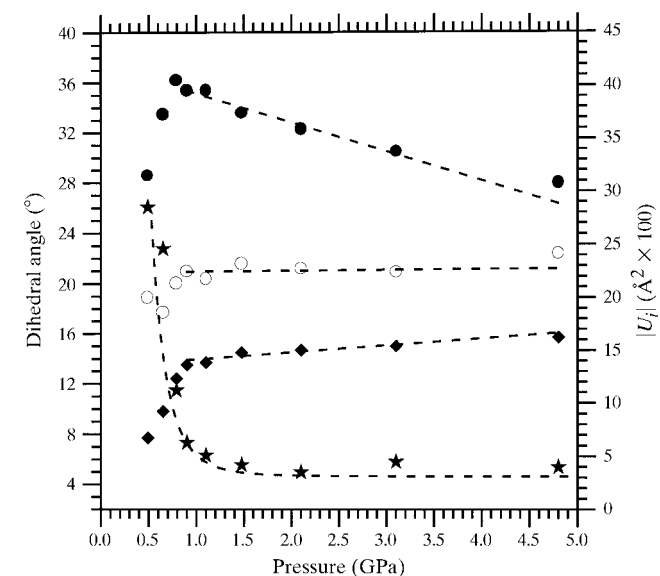


Figure 5 Temperature factor (right scale) and the three angles defining the conformation of TC (left scale) as a function of pressure. The open circles denote the deviation of the torsion angle of the trimethylsilyl groups of TC located around the [111] axis from the staggered conformation. The closed circles denote the deviation of the torsion angle of the second crystallographically distinct trimethylsilyl group of TC from the staggered conformation. The filled diamonds define the orientation of the molecule, described by the rotation of the projection of the C0–Si2 bond of the second trimethylsilyl group in the (111) plane around the [111] axis. Below 0.9 GPa the different parameters have large standard deviations and are highly correlated. Dashed lines correspond to results of linear regression between 0.9 and 4.8 GPa for the three angles, and of an empirical function of the type $f(x) = a + b(x + c)^d$ for the temperature factor (filled stars) over the entire range of pressure.

cooperate twist exists as in the gas phase, whereas the change from molecular *T* to C3 structure occurs in phase III. In this case there must be a significant jump for both twist angles. Assuming for a moment that this change is not abrupt at high pressure, one would expect a steep but continuous increase of the value of the twist angles within the high-pressure phase III, which is in agreement with the experiment (Fig. 5). This would also presuppose a certain amount of disorder in the high-pressure phase III below 0.49 GPa, which would explain the unusual high overall temperature factor in that pressure region. It should be noted that the variance–covariance matrix does not show any serious correlation between the temperature factor and the twist angles.

Alternatively, the entropic contribution to the free energy is different at different temperatures, and this might be responsible for different structures with the same lattice parameter at low temperature and at high pressures, respectively.

The nearest-neighbour distance between C atoms of the methyl groups of different molecules shows a non-linear behaviour in the pressure range between 0.65 and 4.8 GPa which could be modelled by the empirical function $C-C$ (Å) = $2.548 + (P - 0.619)^{-0.083}$ (GPa) (Fig. 6). By adding H atoms at calculated positions, a minimum distance between the TC molecules of 1.7 Å at 0.8 GPa and of 1.4 Å at 4.8 GPa is obtained. These values are significantly below the expected value of 2.1 Å. A further reduction of the C–C distance would inevitably destroy the crystal structure in the present form (Fig. 7), possibly leading to the loss of long-range order. In such a case only the centres of the TC molecules would contribute to long-range order, leading to a cubic-close-packing (c.c.p.) structure. The latter is observed for phase IV.

Although several analogies exist between quasispherical TC and spherical C_{60} regarding the size of the molecules and the symmetry of the different phases in the solid (Dinnebier *et al.*, 1999), there are distinct differences in the compressibility of the two materials. The bulk modulus of crystalline C_{60} , $K(C_{60}) = 14$ GPa (Sundqvist, 1999), is about twice that of TC. This can be explained by the high molecular rigidity and

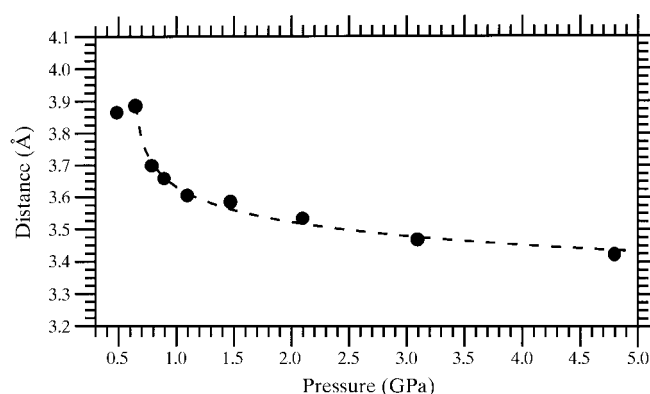


Figure 6 Minimum intermolecular C–C distance between TC molecules in the high-pressure phase III as a function of pressure. The dashed line corresponds to results of an empirical function of the type $f(x) = a + (x + c)^d$ between 0.65 and 4.8 GPa.

stiffness of C_{60} in contrast to TC, which has several intramolecular degrees of freedom. This is also reflected in the phase transitions. Whereas the C_{60} molecule shows reorientations only upon cooling or increasing pressure, there is reorientation and a continuous change in the conformation of the TC molecule.

4. Conclusions

We have found three phase transitions of crystalline tetrakis(trimethylsilyl)methane in the pressure range 0–16 GPa. The compressibility and crystal structures of phase III have been determined in detail for pressures between 0.28 and 4.8 GPa. Our results show that X-ray powder diffraction at a third-generation synchrotron source can be used to refine the crystal structure of a molecular solid at high pressures. The use of rigid bodies for the high-pressure structures was a crucial step for the high-pressure Rietveld refinement, since the constrained atoms shift as a whole and meaningless changes of individual atoms cannot occur. Refinements without or with soft constraints only did not converge to the global minimum due to the limited amount of data available in the powder pattern.

We thank G. Fritz, Karlsruhe, for the donation of the TC sample. We are grateful to Ross Angel (Bayerisches Geoinstitut, Bayreuth) for helpful discussions, and Mohamed Mozouar (ESRF) for kind assistance during the measurements. Research was carried out in part at the European Synchrotron Radiation Facility (ESRF). Financial support by the Deutsche Forschungsgemeinschaft (DFG) is gratefully acknowledged (Di687-2).

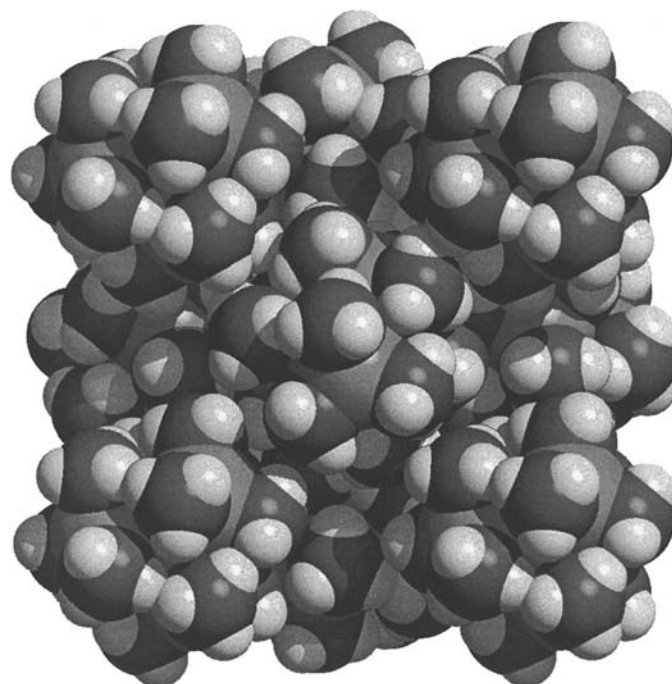


Figure 7 Cup model of the crystal structure of TC at 4.8 GPa.

References

- Aliev, A. E., Harris, K. D. M. & Apperley, D. C. (1993). *J. Chem. Soc. Chem. Commun.* pp. 251–253.
- Aliev, A. E., Harris, K. D. M., Apperley, D. C. & Harris, D. M. (1994). *J. Solid State Chem.* **110**, 314–320.
- Angel, R. J. (1999). *EOSFIT*. Version 4.2. Personal communication.
- Angel, R. J. & Vaughan, M. (2000). *Equations of State, Mineralogical Society of America, Reviews of Mineralogy*, Vol. 3, *Comparative Crystal Chemistry*, ch. 8, edited by R. M. Hazen. Mineralogical Society of America. In the press.
- Bartell, L. S., Clippard, F. B. Jr & Boates, T. L. (1970). *Inorg. Chem.* **9**, 2436–2439.
- Beagley, B., Pritchard, R. G. & Titiloye, J. O. (1988). *J. Mol. Struct.* **176**, 81–87.
- Beagley, B., Pritchard, R. G. & Titiloye, J. O. (1989). *J. Mol. Struct.* **212**, 323–324.
- Birch, F. (1947). *Phys. Rev.* **71**, 809–824.
- Dereppe, J. M. & Magill, J. H. (1972). *J. Phys. Chem.* **76**, 4037–4039.
- Dinnebier, R. E., Dollase, W. A., Helluy, X., Kümmerlen, J., Sebald, A., Schmidt, M. U., Pagola, S., Stephens, P. W. & van Smaalen, S. (1999). *Acta Cryst.* **B55**, 1014–1029.
- Hammersley, A. P., Svensson, S. O., Hanfland, M., Fitch, A. N. & Hausermann, D. (1998). *High Press. Res.* **14**, 235–248.
- Helluy, X., Kümmerlen, J. & Sebald, A. (1998). *Organometallics.* **17**, 5003–5008.
- Iroff, L. D. & Mislow, K. (1978). *J. Am. Chem. Soc.* **100**, 2121–2126.
- Larson, A. C. & Von Dreele, R. B. (1994). *GSAS – General Structure Analysis System*. Report LAUR 86–748. Los Alamos National Laboratory, USA. (Available by anonymous FTP from mist.lanl.gov.)
- Letoullec, R., Pinceaux, J. P. & Loubeyre, P. (1988). *High Press. Res.* **1**, 77–90.
- Mao, H. K., Xu, J. & Bell, P. M. (1986). *J. Geophys. Res.* **91**(B5), 4673–4676.
- Parsonage, N. G. & Staveley, L. A. K. (1978). *Disorder in Crystals*. Oxford: Clarendon.
- Sundqvist, B. (1999). *Adv. Phys.* **48**, 1–134.
- Thompson, P., Cox, D. E. & Hastings, J. B. (1987). *J. Appl. Cryst.* **20**, 79–83.
- Thoms, M., Bauchau, S., Hausermann, D., Kunz, M., Le Bihan, T., Mezouar, M. & Strawbridge, D. (1998). *Nucl. Instrum. Methods Phys. Res. A*, **413**, 175–184.
- Vinet, P., Ferrante, J., Smith, J. R. & Rose, J. H. (1986). *J. Phys. C*, **19**, L467–473.